Rotational Spectrum and Structure of the $(OCS)_2-CO_2$ Trimer

Sean A. Peebles and Robert L. Kuczkowski*

Department of Chemistry, The University of Michigan, 930 North University Avenue, Ann Arbor, Michigan 48109-1055

Received: June 8, 1998; In Final Form: August 7, 1998

The rotational spectra of seven isotopes of the $CO_2-(OCS)_2$ mixed trimer have been assigned using pulsed nozzle FTMW spectroscopy techniques. The structure resembles a distorted triangular cylinder with the three monomers aligned roughly parallel. The trimer may be thought of as a slightly perturbed $(OCS)_2$ dimer with the CO_2 lying above the dimer and crossed at 12° and 20° to the axes of the two OCS molecules, respectively. The distance between the carbon atoms on the OCS is 3.757(9) Å. The distance between the carbon on each OCS and the carbon on the CO_2 is 3.574(6) and 3.773(8) Å, respectively. The dipole moment components for the trimer are $\mu_a = 0.40(1)$ D, $\mu_b = 0.21(7)$ D, and $\mu_c = 0.206(1)$ D with $\mu_{total} = 0.50(4)$ D. The structure and dipole moments are close to those predicted by an interaction model which includes a distributed multipole moment electrostatic contribution and atom−atom terms to describe the dispersion and repulsion interactions.

Introduction

In the past decade a growing number of studies of the structures of weakly bound trimers have been carried out by high-resolution spectroscopy. These provide a necessary resource for developing and testing models that seek to characterize intermolecular interactions. Since ab initio methods are generally less amenable to the study of larger weakly bonded systems, semiempirical methods are often employed in an attempt to rationalize and quantify the structures. Semiempirical models based on distributed electrostatic interactions, such as the Buckingham−Fowler model,[1,2] taken together with formulations to include dispersion−repulsion interactions,[3−7] have often proven to be qualitatively accurate in the case of dimers, although the shortcomings of the less-sophisticated representations of the interaction potential may become apparent when applying these models to the study of larger systems. For any model to accurately characterize intermolecular interactions, it must be able to quantify the effects of a third body on the interaction between two molecules, and this is where the data accumulated from the studies of trimer systems can play a valuable role. From the growing number of trimers that have already been classified, it is becoming apparent that trimers are often composed of sets of dimer-type structures, although with subtle differences in the angles and/or lengths. Attempting to explain and rationalize trimer properties by comparison to dimer interactions can, therefore, provide a worthwhile challenge and aid in the development of more complex models.

The rotational spectrum of the $(CO_2)_2-OCS$ trimer was recently assigned in this laboratory,[8,9] and in this paper we present the determination of the structure of the other mixed trimer $CO_2-(OCS)_2$. Although the dimer-type interactions that are observed in the OCS dimer[10] and the CO_2-OCS dimer[11] are both clearly present in the $CO_2-(OCS)_2$ trimer, the trimer structure has important differences that will be discussed in this paper.

Experimental Section

The rotational spectrum of the $CO_2-(OCS)_2$ trimer was observed using a Balle−Flygare-type Fourier transform microwave spectrometer[12] in the 5.5−10 GHz frequency range. The $CO_2-(OCS)_2$ spectrum was assigned from lines remaining from the initial searches for the $(CO_2)_2-OCS$ trimer.[8,9] These searches covered a region of approximately 2 GHz and were made possible by the recent upgrading of the Michigan spectrometer[13] to an autoscan mode using software and hardware developments from the University of Kiel.[14] Stark-effect measurements to determine the dipole moment components of the complex were conducted by the application of voltages up to ±9 kV to a pair of parallel 50 cm × 50 cm steel mesh plates that are situated inside the evacuated Fabry−Pérot cavity and separated by about 30 cm. Calibration of the electric field was carried out daily using the $J = 1 \leftarrow 0$ transition of OCS at 12162.980 MHz and assuming a dipole moment of 0.7152 D.[15]

The $CO_2-(OCS)_2$ trimer was generated in a supersonic expansion using a gas mixture comprising approximately 1.5% OCS and 1.5% CO_2 seeded in a 97% He−Ne "first-run" mixture (90% Ne, 10% He). The back-pressure of the He−Ne carrier was kept around 2.5−3 atm in order to achieve optimum line intensity. The He/Ne/OCS/CO_2 mixture was expanded into the evacuated cavity through a modified Bosch fuel injector valve, perpendicular to the direction of microwave propagation, with gas and microwave pulse timings set to minimize Doppler broadening. Line widths were approximately 30 kHz full-width at half-maximum, and our transition frequencies were reproducible to around 2 kHz for the strongest of the observed trimer lines. The smaller dipole moment components for this species (compared to the $(CO_2)_2-OCS$ trimer) resulted in slightly weaker lines, which necessitated averaging over several thousand shots (typically 4000) for some of the less-intense transitions in the mixed isotopomers. The $5_{05}-4_{04}$ transition for the normal species was, however, easily observed at an optimum signal-to-noise ratio of 3.5 in 100 gas pulses. No evidence of any splitting in the transitions was seen in any of the measurements.

$^{13}CO_2$ (99% ^{13}C, Isotec) and $C^{18}O_2$ (97.55% ^{18}O, Icon) were used to observe the $^{13}CO_2-(OCS)_2$ and $C^{18}O_2-(OCS)_2$ spectra. Mixtures (1:1:2) of ^{16}OCS, ^{18}OCS (93.4% ^{18}O, Isotec), and CO_2 were prepared to observe the spectra of the two singly

S1089-5639(98)02540-7 CCC: $15.00
Published on Web 09/26/1998

substituted $CO_2-{}^{16}OCS-{}^{18}OCS$ isotopomers. Likewise, 1:1:2 mixtures of $O^{12}CS$, $O^{13}CS$ (99% ^{13}C , Isotec), and CO_2 were prepared to observe the two possible singly substituted $CO_2-O^{12}CS-O^{13}CS$ isotopomers. Attempts to locate the singly substituted $C^{16}O^{18}O$ isotopomer were unsuccessful. Mixing of equal amounts of $C^{18}O_2$ and $C^{16}O_2$ supposedly leads[16] to quick exchange to give a 1:2:1 statistical mixture of $C^{16}O_2$:$C^{16}O^{18}O$:$C^{18}O_2$. Searches of the regions expected to contain the transitions for both of the possible isotopomers revealed no likely transitions. Addition of a small amount of SO_2 to the sample bulb allowed the observation of known $C^{16}O^{18}O{\cdot}SO_2$ transitions[16] to allow us to track the $C^{16}O^{18}O$ concentration. Comparison of the intensity of a $C^{16}O^{18}O{\cdot}SO_2$ transition with that of the normal isotopomer revealed at least 2 orders of magnitude difference. In the case of the more intense lines of the $SO_2{\cdot}CO_2$ spectrum, this was a minor inconvenience, but in the $(OCS)_2CO_2$ system, where the lines were already weak, this reduced intensity results in lines too weak for us to see in reasonable numbers of shots. We can only conclude, therefore, that the amount of $^{16}O-{}^{18}O$ random scrambling that we have encountered is modest and that the concentration of the $C^{16}O^{18}O$ species in our samples is very low. This low isotopic concentration coupled with insufficient isotopic supplies and the current low commercial availability of ^{18}O isotopic species prevented us from pursuing the assignment of the $C^{16}O^{18}O$-containing species.

Results

A. Spectra. *a*-, *b*-, and *c*-type transitions were observed for all of the isotopic species, with the *a*-type lines being the most intense. Measured frequencies for the 42 transitions belonging to the normal species $CO_2-(OCS)_2$ are listed in Table 1, along with the residuals of a fit of these lines to a Watson A-reduced Hamiltonian in the I^r representation. Spectra for the following isotopically substituted species were also observed: $^{13}CO_2-(OCS)_2$, $C^{18}O_2-(OCS)_2$, $CO_2-O^{13}CS-O^{12}CS$, $CO_2-O^{12}CS-O^{13}CS$, $CO_2-{}^{18}OCS-{}^{16}OCS$, and $CO_2-{}^{16}OCS-{}^{18}OCS$. The fitted rotational and centrifugal distortion constants for the normal and all of the isotopic species are listed in Tables 2 and 3. The value of Δ_{JK} was held fixed at zero in the fits of the isotopic species since it was poorly determined and its inclusion led to no noticeable difference in the fit. Transition frequencies for the isotopic species are available as Supporting Information.

B. Dipole Moment. The analysis of the Stark effects of six rotational transitions (for a total of eight components) was able to provide good-quality dipole moment data. Table 4 lists the observed Stark coefficients and the computed dipole moment components. The dipole components were computed to be $|\mu_a| = 0.405(6)$ D, $|\mu_b| = 0.21(7)$ D, and $|\mu_c| = 0.2056(8)$ D. The total dipole moment $\mu_{tot} = 0.50(4)$ D is 0.2 D less than the dipole moment of a single OCS monomer (0.7152 D[15]) and suggests that the two OCS dipoles are aligned in some way such as to partially cancel. The much higher uncertainty in the magnitude of the μ_b component arises from the very small contribution that this component makes to the measured frequency shifts in the transitions studied.

C. Structure. Experimental rotational constants for the normal species and six other isotopic species provided sufficient isotopic data to allow a reasonably well-determined structure to be obtained. Singly substituted isotopic data for all three carbon atoms and the oxygen atoms of the two OCS molecules enabled Kraitchman coordinates to be calculated[17] for these atoms, effectively fixing the positions of the three carbon atoms and the relative orientations of the OCS molecules in the trimer. The absolute values of the substitution structure coordinates are given in parentheses in Table 5, along with the coordinates that result from the inertial fit.

The location of the oxygen atoms of CO_2 proved to be more difficult. The ^{13}C single-substitution data provided the position of the carbon atom, but the $C^{18}O_2$ isotopic data did not readily locate the oxygen atoms using our structure fitting programs. Searches for the $C^{16}O^{18}O$ species proved fruitless (as described in the Experimental Section). Consequently, an iterative process was devised to ascertain the best structure from the available data. Nine parameters are needed to define the structure of the trimer. The parameters actually fitted were the two carbon−carbon distances $r(C_1-C_7)$ and $r(C_4-C_7)$, the four angles $(C_1-C_7-C_4)$, $(C_7-C_4-O_5)$, $(C_1-C_7-O_8)$, and $(C_4-C_1-O_2)$, and the three dihedral angles $(O_2-C_1-C_4-C_7)$, $(O_5-C_4-C_7-C_1)$, and $(O_8-C_7-C_1-C_4)$. Efforts to fit all nine parameters to the 21 moments of inertia by least-squares techniques using Schwendeman's STRFITQ program[18] did not converge due to linear dependencies in the equations. However, fixing one parameter viz β ($O_8-C_7-C_1-C_4$, see Figure 1) gave convergence and determination of the remaining eight parameters. This was repeated for a range of values for the angle β with the optimum

TABLE 1: Observed Rotational Transitions (MHz) for the Normal Isotopomer of the $CO_2-(OCS)_2$ Trimer

$J_{K_aK_c'}$	$J_{K_aK_c''}$	ν_{obs}/MHz	$\Delta\nu$/kHz[a]
3_{30}	2_{20}	5798.1604	0.2
3_{31}	2_{21}	5883.0940	−5.5
4_{23}	3_{22}	5772.5810	5.9
4_{13}	3_{12}	5901.7680	0.5
4_{23}	3_{12}	5952.0669	1.2
4_{32}	3_{31}	6134.7111	5.4
4_{22}	3_{21}	6479.6880	1.2
4_{31}	3_{30}	6484.0621	1.0
4_{22}	3_{12}	7295.7644	0.5
4_{31}	3_{21}	7377.5857	0.5
4_{13}	3_{03}	7440.1525	−1.5
4_{23}	3_{13}	7482.8546	−5.8
4_{32}	3_{22}	7575.5460	3.0
4_{41}	3_{30}	7786.7648	−5.3
4_{41}	3_{31}	7876.0470	3.6
4_{31}	3_{22}	7014.1744	2.7
4_{22}	3_{13}	8826.5610	2.5
5_{05}	4_{14}	6383.9960	−0.3
5_{15}	4_{14}	6384.1707	3.1
5_{05}	4_{04}	6385.1925	−4.5
5_{15}	4_{04}	6385.3687	0.4
5_{14}	4_{23}	7020.8559	0.6
5_{24}	4_{23}	7031.2866	2.5
5_{14}	4_{13}	7071.1575	4.0
5_{24}	4_{13}	7081.5821	−0.3
5_{23}	4_{32}	7371.3647	−7.1
5_{33}	4_{32}	7551.2169	−5.4
5_{42}	4_{41}	7775.7186	−0.4
5_{23}	4_{22}	7830.6349	−6.6
5_{41}	4_{40}	7994.6417	−4.5
5_{33}	4_{22}	8010.4922	0.2
5_{32}	4_{31}	8199.4963	0.9
5_{32}	4_{22}	9097.3951	1.3
5_{23}	4_{13}	9224.6393	1.3
6_{16}	5_{15}	7595.0786	9.0
6_{06}	5_{05}	7595.2077	−10.3
6_{15}	5_{14}	8263.6176	1.0
6_{34}	5_{33}	8869.9577	5.2
6_{24}	5_{23}	9000.9481	−2.3
6_{52}	5_{51}	9377.0151	−1.0
6_{33}	5_{32}	9707.4790	2.0
6_{42}	5_{41}	9814.1839	1.1

[a] $\Delta\nu = \nu_{obs} - \nu_{calc}$.

TABLE 2: Spectroscopic Constants for the Normal and ^{13}C-Enriched Isotopomers

spectroscopic constant	$CO_2-(OCS)_2$	$CO_2-O^{12}CS-O^{13}CS$	$CO_2-O^{13}CS-O^{12}CS$	$^{13}CO_2-(OCS)_2$
A/MHz	1010.7197(8)	1006.7130(19)	1002.2181(15)	1007.4972(6)
B/MHz	875.4035(3)	872.2051(9)	875.3363(7)	868.5808(3)
C/MHz	605.3805(4)	602.7212(9)	602.3492(7)	601.5318(4)
Δ_J/kHz	0.877(4)	0.816(14)	0.768(11)	0.847(5)
Δ_{JK}/kHz	−0.198(26)	*a*	*a*	*a*
Δ_K/kHz	1.41(4)	1.3(2)	1.48(16)	1.25(4)
δ_J/kHz	0.207(3)	0.188(8)	0.202(6)	0.191(3)
δ_K/kHz	0.41(1)	0.33(4)	0.36(4)	0.41(1)
$\Delta\nu_{rms}$/kHz[b]	3.86	5.33	4.02	3.42
N[c]	42	25	24	38

[a] Δ_{JK} was not well-determined for these isotopes. The value was fixed at zero with no significant effect on the fits. [b] $\Delta\nu_{rms} = [\sum(\nu_{obs} - \nu_{calc})^2/N]^{1/2}$. [c] *N* is the number of fitted transitions.

TABLE 3: Spectroscopic Constants for the ^{18}O-Enriched Isotopomers

spectroscopic constant	$C^{18}O_2-(OCS)_2$	$CO_2-^{16}OCS-^{18}OCS$	$CO_2-^{18}OCS-^{16}OCS$
A/MHz	994.1089(6)	983.7085(12)	992.7163(11)
B/MHz	841.1981(3)	870.5506(6)	871.9423(6)
C/MHz	588.9154(4)	597.1630(5)	599.7929(6)
Δ_J/kHz	0.797(5)	0.842(10)	0.798(9)
Δ_K/kHz	1.00(3)	0.91(12)	1.59(12)
δ_J/kHz	0.187(3)	0.186(5)	0.160(5)
δ_K/kHz	0.51(1)	0.37(3)	0.38(3)
$\Delta\nu_{rms}$/kHz[a]	3.35	3.44	3.31
N[b]	38	24	24

[a] $\Delta\nu_{rms} = [\sum(\nu_{obs} - \nu_{calc})^2/N]^{1/2}$. [b] *N* is the number of fitted transitions.

TABLE 4: Stark Coefficients and Dipole Moments for $CO_2-(OCS)_2$

transition	$\|M\|$	$\Delta\nu/\epsilon^{2a}$	obsd − calcd[a]
$4_{13}-3_{12}$	1	−0.295	0.000
	2	−1.160	−0.001
$4_{23}-3_{13}$	1	−8.275	−0.015
$4_{31}-3_{30}$	1	−2.507	−0.062
$4_{41}-3_{31}$	1	−1.326	0.107
$5_{14}-4_{13}$	1	−1.414	−0.103
	2	−5.181	0.054
$5_{24}-4_{23}$	1	1.347	0.015
	$\mu_a = 0.405(6)$ D		
	$\mu_b = 0.21(7)$ D		
	$\mu_c = 0.2056(8)$ D		
	$\mu_{tot} = 0.50(4)$ D		

[a] Observed Stark coefficients and residuals in units of 10^{-5} MHz/(V cm^{-1})^2.

TABLE 5: Principal Axis Coordinates Determined from a Least-Squares Fit of the Inertial Data (Å)[a]

atom[b]	*a*	*b*	*c*
C_1	0.04891	2.05879	0.20495
	|0.04316|	|2.05188|	|0.20776|
C_4	−1.37246	−1.35454	−0.45910
	|1.36574|	|1.35113|	|0.46384|
C_7	2.01710	−1.12875	0.65188
	|2.01999|	|1.12644|	|0.63584|
M_1	0.29146	1.92066	−0.24099
O_2	−0.48411	2.36231	1.18491
	|0.45794|	|2.35183|	|1.19993|
S_3	0.77049	1.64788	−1.12170
M_4	−1.77114	−1.09265	−0.23721
O_5	−0.49634	−1.93007	−0.94670
	|0.47713|	|1.91654|	|0.96523|
S_6	−2.55852	−0.57541	0.20101
O_8	1.25771	−0.79718	1.46652
O_9	2.77649	−1.46032	−0.16276

[a] Absolute values in brackets for the carbons of CO_2 and the C and O atoms of OCS are the Kraitchman substitution coordinates obtained from the single isotopic substitution data. [b] See Figure 1 for the atom numbers. (M_1 and M_4 are the centers of mass of the OCS molecules and are bound to C_1 and C_4, respectively).

fit (as judged by ΔI_{rms}) resulting when β is fixed at −79°. The parameters from the geometry that best fit the inertial data are given in Table 6. The deviation of the fit ($\Delta I_{rms} = 0.119$ amu Å^2) is reasonably good, with the data from the $C^{18}O_2$ isotopomer having the largest deviation.

During the least-squares fitting, the monomer geometries were held fixed at their literature values (r(C−O) = 1.162 Å in CO_2;[19] r(C−O) = 1.1561 Å, and r(C−S) = 1.5651 Å in OCS[20]). Calculation of the O−C bond lengths in the OCS molecules from the single isotopic substitution data leads to lengths of 1.167 and 1.116 Å, in good agreement with the literature value of 1.156 Å.

The principal axis coordinates resulting from the least-squares fitting of the inertial data are given in Table 5. It can be seen from the table that the coordinates derived from the inertial fit are in good agreement with those obtained from the Kraitchman calculations on the singly substituted isotopomers. Table 6 lists the structural parameters calculated from the coordinates given in Table 5, as well as parameters obtained from a semiempirical model, which will be discussed later.

The structural parameters from the inertial fit are obtained by fitting ground-state moments of inertia and, hence, ignore any vibrational contributions to those moments. The uncertainties listed in Table 6 are statistical uncertainties that arise from the fitting process and do not take into account any errors that may arise from a neglect of the vibrational effects in this model. These errors cannot be estimated without some information on the vibrations, which is beyond the scope of this study. However, it is possible to conclude that the derived parameters are a reasonable approximation to the structure: the consistency of the fit for the isotopic species, small centrifugal distortion constants, good agreement between the Kraitchman coordinates and those from the inertial fit and with the resulting monomer bond distances, and the absence of any tunneling splittings in

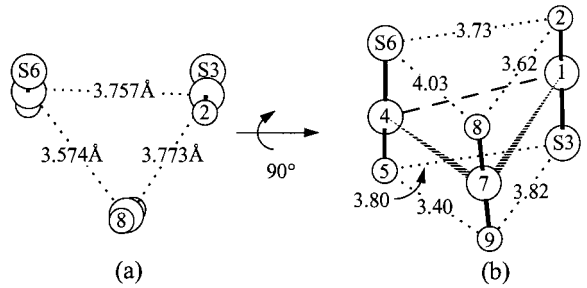

Figure 1. Interatomic distances in the $CO_2-(OCS)_2$ trimer. The perspective in a places the carbon of the left-hand OCS in the plane of the paper, the carbon of the right-hand OCS slightly behind this plane, and the carbon of the CO_2 slightly in front of the plane. The perspective in b is obtained by rotating a by 90° about the arrow, placing C_1 and C_4 in the plane of the paper and C_7 above the plane. All distances are in angstroms.

TABLE 6: Comparison of Calculated Structural Parameters for the $CO_2-(OCS)_2$ Trimer

parameter	inertial fit	Kraitchman (r_s)	model[a]
$r(C_1-C_7)$/Å	3.773(8)	3.767	3.795
$r(C_4-C_7)$/Å	3.574(6)	3.567	3.588
$r(C_1-C_4)$/Å	3.757(9)	3.744	3.695
$r(C_7-M_1)$/Å	3.616(9)		3.627
$r(C_7-M_4)$/Å	3.891(8)		3.905
$r(M_1-M_4)$/Å	3.652(12)		3.508
$\angle(C_4-C_7-C_1)$/deg	61.4(1)		60.0
$\angle(O_5-C_4-C_7)$/deg	56.2(7)		56.2
$\angle(O_2-C_1-C_4)$/deg	102.3(4)		107.8
$\angle(O_8-C_7-C_1)$/deg	60.1(14)		52.4
$\tau(O_5-C_4-C_7-C_1)$/deg[b]	133.2(9)		138.4
$\tau(O_2-C_1-C_4-C_7)$/deg[b]	−107.4(7)		−105.6
$\tau(O_8-C_7-C_1-C_4)$/deg[b]	−79.0		−71.2

[a] Calculated from the ORIENT model predictions, using the electrostatic + dispersion/repulsion potential. [b] Signs of the dihedral angles are consistent with the definition in ref 32.

the rotational spectra. It is reasonable to assume that the equilibrium parameters would fall within ±0.05 Å and ±5° of the values given in the tables and figures.

Discussion

Figures 1 and 2 clearly show that the $CO_2-(OCS)_2$ trimer has the same cylinder-like shape that was recently observed for the $(CO_2)_2-OCS$ trimer.[8,9] The structure is barrel-shaped, with the three monomer units aligned roughly parallel to one another. The OCS dimer portion of the trimer is quite clearly no longer planar, with considerable out-of-plane tilts of the O and S atoms. It is this tilting and twisting of the OCS molecules relative to one another that is principally responsible for making this trimer polar, thus enabling its structure determination by microwave techniques. The center of mass separation in the OCS dimer fragment in the trimer is calculated to be 3.652 Å, effectively unchanged from the value of 3.648 Å in the dimer.[10] Figures 3 and 4 compare the structural parameters within the respective dimer-like fragments that comprise the trimer. From Figure 3 it is clear that the perturbation of the $(OCS)_2$ portion of the trimer is very small. The increase in the C−C distance of around 0.05 Å and changes of only a couple of degrees in the planar angles on going from the isolated dimer to the trimer both show minimal variation from their values in the dimer. The most significant change upon formation of the trimer is that the $(OCS)_2$ fragment is no longer planar. In Figure 3a the dihedral angle O−C···C−S is necessarily 0° for a planar configuration. In Figure 3b the angle $O_5-C_4\cdots C_1-S_3$ is calculated to be 34.0°, a significant departure from planarity.

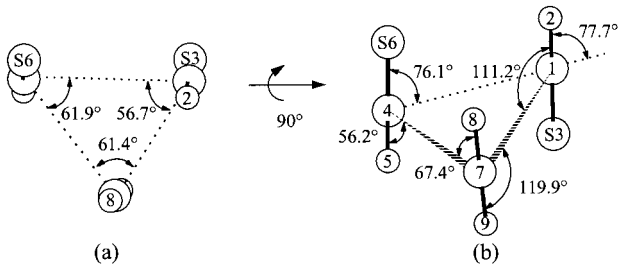

Figure 2. Planar angles in the $CO_2-(OCS)_2$ trimer. The perspective in a is the same as in Figure 1a. (b) Obtained by a 90° rotation about the arrow.

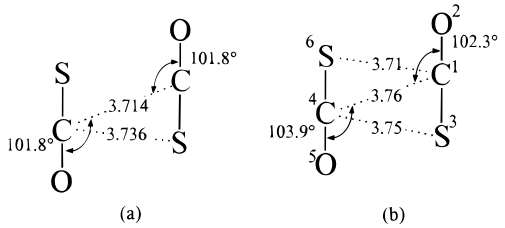

Figure 3. Comparison of (a) the OCS dimer and (b) the OCS dimer face in the $CO_2-(OCS)_2$ trimer. Distances are in angstroms.

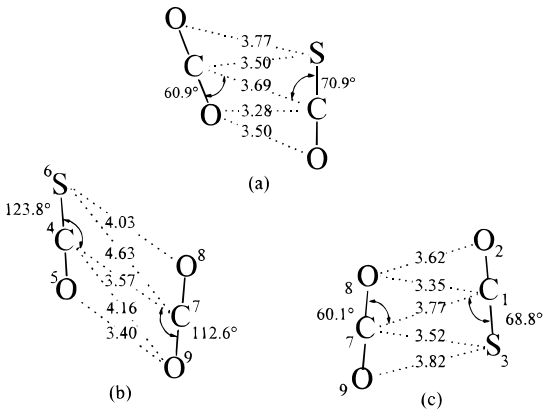

Figure 4. Comparison of (a) the CO_2-OCS dimer with (b,c) the CO_2-OCS faces in the $CO_2-(OCS)_2$ trimer. Distances are in angstroms.

Interestingly, the sign of the dihedral angle is such that the sulfur atoms move away from the CO_2 (Figure 1).

Comparison of the two CO_2-OCS faces of the trimer in Figure 4 (b and c) reveals a more striking departure from the CO_2-OCS dimer structure. The CO_2-OCS face of the trimer illustrated in Figure 4b is significantly different from the dimer structure of Figure 4a. The C−C distance of 3.57 Å in this case represents a 0.12 Å decrease from the dimer. An inspection of the planar angles in Figure 4b reveals the extent to which it differs from the dimer, with the angles being approximately 50° different from the respective angles in the dimer. In contrast, the CO_2-OCS face in Figure 4c resembles the dimer structure of Figure 4a quite closely, with the C−C distance of 3.77 Å representing an increase of just 0.08 Å with respect to the dimer. The planar angles are, like those in the $(OCS)_2$ fragment, little different from the dimer, differing only by up to 2°. The planarity of the CO_2-OCS fragment is lost in the trimer, with the dihedral angle $O_9-C_7\cdots C_1-S_3$ calculated to be 12.1°. This is consistent with similar observations in the related $(CO_2)_2-OCS$ trimer[8,9] where one CO_2-OCS face closely reproduced the structural parameters of the dimer while the other face had angles that differed by 40−50° from those of the dimer. Once again, the CO_2-OCS fragment is no longer planar; the dihedral angle $O_8-C_7\cdots C_4-S_6$ is calculated to be 20.4°.

TABLE 7: Distributed Multipole Moments for CO_2 and OCS[a]

molecule	atom	z	Q_{00}	Q_{10}	Q_{20}	Q_{30}	Q_{40}
CO_2	C	0.0	1.3975	0.0	−0.2773	0.0	1.9108
	O_1	2.19587	−0.6988	0.3949	−0.1688	0.2869	−0.2226
	O_2	−2.19587	−0.6988	−0.3949	−0.1688	−0.2869	−0.2226
OCS	C	0.0	0.6459	−0.4583	0.2874	1.7532	7.0876
	O	−2.18471	−0.5191	−0.0835	0.2768	0.4369	0.7085
	S	2.95761	−0.1268	0.0801	1.6594	−0.7748	2.3408

[a] All quantities are in atomic units.

TABLE 8: Comparison of Experimental and Predicted Constants for $CO_2-(OCS)_2$

constant	expl	predicted[a] (exp-6)	predicted[a] (pseudo-hard-sphere)
A/MHz	1010.7197(8)	1061.872	1299.246
B/MHz	875.4035(3)	880.912	604.985
C/MHz	605.3805(4)	613.880	451.937
μ_a/D	0.405(6)	0.31	0.00
μ_b/D	0.21(7)	0.09	0.34
μ_c/D	0.2056(8)	0.36	0.00

[a] The predicted rotational constants were obtained from the ORIENT program using either an atom−atom representation (exp-6) of the dispersion−repulsion term or a pseudo-hard-sphere repulsion potential (see text for discussion). The predicted dipole was obtained from projection of the OCS monomer dipole of the model structure (recovered from the distributed multipole moments for that molecule) into the principal axis system.

The initial assignment of this species from the lines that remained after assignment of the $(CO_2)_2-OCS$ trimer spectrum was guided by predictions from a structure obtained from a theoretical model. The success of the ORIENT program[21] in closely reproducing the geometry of the $(CO_2)_2-OCS$ trimer led us to model the $(OCS)_2-CO_2$ trimer in an attempt to obtain sufficiently good rotational constants to help identify the unassigned lines. Anthony Stone's ORIENT program[21] employs distributed multipole moments to describe the electrostatic term in the intermolecular interaction potential and utilizes an analytical dispersion and repulsion term. Distributed multipole moments for CO_2 and OCS were calculated at the SCF level from the CADPAC suite of programs[22] using a TZ2P basis set from the CADPAC library. Moments up to and including hexadecapoles were calculated on each atom site and are listed in Table 7. The inclusion of dispersion and repulsion interactions in the potential is achieved by means of atom−atom terms of the exp-6 type. For instance, for an interaction between two molecules A and B, we can represent the combined dispersion and repulsion energy by the expression[23]

$$U_{\text{exp}-6} = \sum_{i,j} K \exp[-\alpha_{ij}(R_{ij} - \rho_{ij})] - \frac{C_6^{ij}}{R_{ij}^6} \qquad (1)$$

where i and j represent sites on molecules A and B, respectively, and R_{ij} is the distance between these sites. α_{ij} describes the hardness of the repulsion and is dependent upon a particular site pair. ρ_{ij} is the sum of the effective radii of the atoms, and C_6^{ij} is an empirical site−site dispersion term. K is a convenient energy unit, taken to be 10^{-3} E_h (hartree) in the present work, which corresponds to an approximate temperature of 316 K. This makes it suitable for the description of interactions at ambient temperatures. ρ_{ij} will then be the distance at which the repulsion energy between sites i and j has a value equal to that of the constant K. Values for α_{ij}, ρ_{ij}, and C_6^{ij} were obtained from the tabulated values of Mirsky[24] and taken from Table 11.2 of ref 23. Values for atom−atom pairs not available in ref 23 were estimated by means of the following combining rules: harmonic mean for α (i.e., $1/\alpha_{ij} \approx 1/\alpha_i + 1/\alpha_j$), arithmetic mean for ρ, and geometric mean for C_6. Using this model, the resulting minimum energy conformation for the $CO_2-(OCS)_2$ trimer was found to be a noncyclic, barrel-like structure in which the three monomers were aligned roughly parallel, with an interaction energy of -1591.7 cm^{-1}. The rotational constants and projected dipole moment components that are predicted from this model are given in Table 8, where they are compared with experimental values and those using a pseudo-hard-sphere repulsion potential to be described below. Structural parameters calculated from the dispersion−repulsion model are listed in Table 6, where they are compared with those from the inertial fit and the Kraitchman single isotopic substitution calculations.

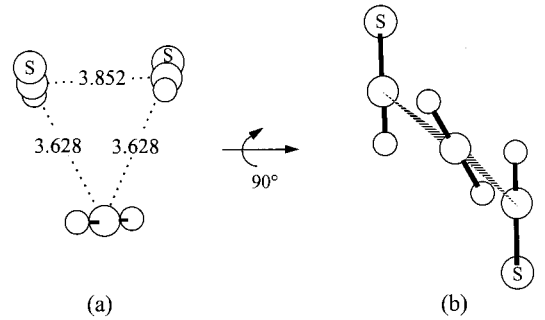

Figure 5. Predicted geometry of the $CO_2-(OCS)_2$ trimer using a pseudo-hard-sphere repulsion model. In perspective a the carbon atom of the CO_2 is in the plane of the paper, the carbon of the left-hand OCS is slightly behind the plane, and the carbon of the right-hand OCS is slightly in front of the plane. The perspective in b is obtained from rotation of a by 90° about the arrow shown, placing the carbons of the OCS in the plane of the paper. Distances are in angstroms.

In addition to modeling of the trimer structure with an analytical dispersion−repulsion term, a hard-sphere repulsion model was employed (i.e., one that includes only the electrostatic and repulsion contributions) in order to test the effectiveness of the standard Buckingham−Fowler model[1,2] when applied to trimers. The program ORIENT has no provision for a separate inpenetrable hard-sphere potential but does allow one to obtain a pseudo-hard-sphere model by the use of a large value of α in the repulsion potential (the default value of 25 a_0^{-1} (bohr^{-1}) for α was used here). ρ is the sum of the site radii, where the site radii are simply the van der Waals radii as tabulated by Pauling.[25] R is the site−site distance, and K is the preexponential factor which may be adjusted to improve the estimation of the intermolecular separation. In this instance, the default value of 0.001 E_h was used.

It was not possible to closely reproduce the cylinder-like structure of the $CO_2-(OCS)_2$ trimer using this pseudo-hard-sphere model, although a global minimum barrel-shaped geometry was observed. In this geometry, the carbon atom of the CO_2 is located almost directly above the midpoint of the line joining the carbon atoms of the OCS molecules (see Figure 5). The C−C distance in the OCS dimer portion of the trimer is predicted to be 3.852 Å, while the distances between the OCS

carbon atoms and the CO_2 carbon atom are both 3.628 Å, all within 0.15 Å of the experimental distances. Only a μ_b dipole component of ~0.34 D is predicted for this geometry; μ_a and μ_c are both approximately zero as a consequence of cancellation of the OCS dipole components in these directions. The rotational constants and dipole moments predicted from this model are given in Table 8, where it can be seen that this model gives a very much poorer reproduction of the structure. The tilt angles of the monomers relative to one another and the relative position of the CO_2 are not predicted as accurately (i.e., in the experimental structure, the CO_2 is found to be moved relative to the OCS dimer fragment such that the oxygen atom rather than the carbon atom of the CO_2 molecule is located near the midpoint of the line joining the two carbon atoms of the OCS molecules). The structure resulting from the pseudo-hard-sphere repulsion model is, at first glance, a reasonable approximation to the true experimental structure. However, a closer inspection of the rotational constants and dipole moment reveals some rather significant differences in the details of the geometry. Although the dispersion−repulsion model still lacks some of the finer details in the angles, the geometry prediction is clearly of sufficient quality that it was extremely useful in the initial assignment of the rotational spectrum. The inclusion of dispersion and a somewhat more realistic representation of the repulsion in the electrostatic−dispersion−repulsion model evidently provides the fine-tuning necessary to bring the predicted structure into almost quantitative agreement with the experimental determination. The small increase in the complexity of the intermolecular interaction potential has, in the cases involving triatomic linear monomers studied so far at least, been rewarded by practical estimates of the geometries of these systems.

Summary

The $CO_2-(OCS)_2$ trimer has been found to possess the tilted barrel shape that has also been observed in a number of trimer systems to date. For example, the three homomolecular trimers $(OCS)_3$,[26] $(CO_2)_3$,[27] and $(N_2O)_3$[28] and the mixed trimers $(CO_2)_2-OCS$[8,9] and $(CO_2)_2-H_2O$[29,30] all possess structures that resemble $CO_2-(OCS)_2$. Only for the $(CO_2)_3$ system has a second, planar-pinwheel isomer also been observed.[31] The $CO_2-(OCS)_2$ structure may be described as having two dimer-like interactions that display minimal deviation from their respective dimer structures (CO_2-OCS and $(OCS)_2$) and another CO_2-OCS interaction which is markedly different from that seen in the dimer. The structure has been closely reproduced by a model incorporating electrostatic, dispersion, and repulsion interactions, suggesting that the basic physics of the interaction can be reasonably well-explained in these terms. It will be interesting to see whether this model is successful in performing with the same level of success for other, relatively simple, termolecular systems of linear triatomics, and further studies along these lines are underway.

Acknowledgment. This work was supported by the Experimental Physical Chemistry Program, National Science Foundation, Washington, DC. We are grateful to the following people for their contributions to the automation of our FTMW spectrometers: Jens-Uwe Grabow, Ioannis Ioannou, Kurt Hillig, and Robb Wilson.

Supporting Information Available: Tables of rotational transition frequencies for the isotopic species (12 pages). Ordering information is given on any current masthead page.

References and Notes

(1) Buckingham, A. D.; Fowler, P. W. *J. Chem. Phys*. **1983**, *79*, 6426.
(2) Buckingham, A. D.; Fowler, P. W. *Can. J. Chem.* **1985**, *63*, 2018.
(3) Muenter, J. S. *J. Chem. Phys.* **1991**, *94*, 2781.
(4) Spackman, M. A. *J. Phys. Chem.* **1987**, *91*, 3179.
(5) Dykstra, C. E. *Chem. Rev.* **1993**, *93*, 2339.
(6) Wales, D. J.; Stone, A. J.; Popelier, P. A. *Chem. Phys. Lett.* **1995**, *240*, 89.
(7) Peebles, S. A.; Kuczkowski, R. L. *J. Mol. Struct.* **1998**, *442*, 151.
(8) Peebles, S. A.; Kuczkowski, R. L. *Chem. Phys. Lett*. **1998**, *286*, 421.
(9) Peebles, S. A.; Kuczkowski, R. L. *J. Chem. Phys.* **1998**, *109*, 5276.
(10) Randall, R. W.; Wilkie, J. M.; Howard, B. J.; Muenter, J. S. *Mol. Phys.* **1990**, *69*, 839.
(11) Novick, S. E.; Suenram, R. D.; Lovas, F. J. *J. Chem. Phys*. **1988**, *88*, 687.
(12) Balle, T. J.; Flygare, W. H. *Rev. Sci. Instrum*. **1981**, *52*, 33.
(13) Hillig, K. W., II; Matos, J.; Scioly, A.; Kuczkowski, R. L. *Chem. Phys. Lett*. **1987**, *133*, 359.
(14) Grabow, J.-U. Ph.D. Thesis, University of Kiel, 1992.
(15) Muenter, J. S. *J. Chem. Phys*. **1968**, *48*, 4544.
(16) Sun, L. H.; Ioannou, I. I.; Kuczkowski, R. L. *Mol. Phys.* **1996**, *88*, 255.
(17) Kraitchman, J. *Am. J. Phys*. **1953**, *21*, 17.
(18) Schwendeman, R. H. In *Critical Evaluation of Chemical and Physical Structural Information*; Lide, D. R., Paul, M. A., Eds.; National Academy of Sciences: Washington, DC, 1974.
(19) Plyler, E. K.; Blaine, L. R.; Tidwell, E. D. *J. Res. Natl. Bur. Stand*. **1955**, *55*, 183.
(20) Morino, Y.; Matsumura, C. *Bull. Chem. Soc. Jpn.* **1967**, *40*, 1095. Maki, A. G.; Johnson, D. R. *J. Mol. Spectrosc*. **1973**, *47*, 226.
(21) Stone, A. J.; Dullweber, A.; Hodges, M. P.; Popelier, P. L. A.; Wales, D. J. *ORIENT: A program for studying interactions between molecules*, Version 3.2; University of Cambridge, 1995.
(22) CADPAC: The Cambridge Analytic Derivatives Package Issue 6, Cambridge, 1995. A suite of quantum chemistry programs developed by Amos, R. D. with contributions from Alberts, I. L.; Andrews, J. S.; Colwell, S. M.; Handy, N. C.; Jayatilaka, D.; Knowles, P. J.; Kobayashi, R.; Laidig, K. E.; Laming, G.; Lee, A. M.; Maslen, P. E.; Murray, C. W.; Rice, J. E.; Simandiras, E. D.; Stone, A. J.; Su, M.-D.; Tozer, D. J.
(23) Stone, A. J. *The Theory of Intermolecular Forces;* Clarendon Press: Oxford, 1996.
(24) Mirsky, K. In *The determination of the intermolecular interaction energy by empirical methods*; Schenk, R., Olthof-Hazenkamp, R., van Koningveld, H., Bassi, G. C., Eds.; Delft University Press: Delft, The Netherlands, 1978.
(25) Pauling, L. *The Nature of the Chemical Bond*, 3rd ed.; Cornell University Press: Ithaca, NY, 1960.
(26) Connelly, J. P.; Bauder, A.; Chisholm, A., Howard, B. J. *Mol. Phys*. **1996**, *88*, 915.
(27) Weida, M. J.; Nesbitt, D. J. *J. Chem. Phys*. **1996**, *105*, 10210.
(28) Miller, R. E.; Pedersen, L. *J. Chem. Phys*. **1998**, *108*, 436.
(29) Peterson, K. I.; Suenram, R. D.; Lovas, F. J. *J. Chem. Phys*. **1989**, *90*, 5964.
(30) Gutowsky, H. S.; Chuang, C. *J. Chem. Phys*. **1990**, *93*, 894.
(31) Fraser, G. T.; Pine, A. S.; Lafferty, W. J.; Miller, R. E. *J. Chem. Phys*. **1987**, *87*, 1502.
(32) Wilson, E. B.; Decius, J. C.; Cross, P. C. *Molecular Vibrations*; McGraw-Hill: New York, 1955.